

Master's Degree in Mechatronic Engineering



**Politecnico
di Torino**

Master's Degree Thesis

**UNSUPERVISED MACHINE
LEARNING ALGORITHMS FOR EDGE
NOVELTY DETECTION**

Supervisors

Prof. Marcello CHIABERGE

Dott. Umberto ALBERTIN

Dott. Gianluca DARA

Candidate

Ariel PRIARONE

03 2024

Acknowledgements

I would like to thank the PoliTO Interdepartmental Centre for Service Robotics (PIC4Ser) for giving me the opportunity to work on this project. The guidance and infrastructure provided by the centre have been invaluable during the development of this work.

To my parents, who have given me everything.
Thank you for always making me believe that anything is possible.
Ai miei genitori, che mi hanno dato tutto.
Grazie per avermi sempre fatto credere che tutto sia possibile.

Ariel

Table of Contents

List of Tables	III
List of Figures	IV
1 Feature Extraction	1
1.1 Reference dataset	1
1.2 Time-domain features	3
1.3 Frequency-domain features	4
1.3.1 Fourier Transform	5
1.3.2 Wavelet Packet Decomposition	11
1.4 Conclusions	14
Bibliography	16

List of Tables

1.1	IMS Test setup [1]	3
-----	--------------------	---

List of Figures

1.1	The test rig used by [1]	2
1.2	“Bearing 3 x” vibration signal from the IMS dataset	2
1.3	All time-domain features for the “Bearing 3 x” vibration signal from the IMS dataset	5
1.4	FFT of the signal with known frequency components	7
1.5	FFT of the signal with known frequency components, and an additive disturbance	7
1.6	FFT of the signal with known frequency components, with a domain that is not an integer multiple of the period	8
1.7	Hann and Hamming windows	8
1.8	FFT of the signal with a domain that is an integer multiple of the period, and preprocessing techniques applied	9
1.9	FFT of the signal with a domain that is not an integer multiple of the period, and preprocessing techniques applied	10
1.10	FFT of the “Bearing 3 x” vibration signal from the IMS dataset, in normal conditions, with preprocessing techniques applied	10
1.11	FFT of the “Bearing 3 x” vibration signal from the IMS dataset, in normal conditions with Hann window preprocessing applied	11
1.12	Wavelet Packet Decomposition of the “Bearing 3 x” vibration signal from the IMS dataset, in normal conditions	12
1.13	Wavelet Packet Decomposition of the “Bearing 3 x” vibration signal from the IMS dataset, in abnormal conditions	13
1.14	Wavelet Packet Decomposition of the “Bearing 3 x” vibration signal from the IMS dataset, in normal conditions	13

Chapter 1

Feature Extraction

Before diving into the novelty detection framework itself, the features to be used need to be defined and extracted from the data. Since our goal is to detect a novel behaviour, we are interested in both “time-domain” and “frequency-domain” features. The former are used to capture the temporal evolution of the signal, while the latter are used to capture the spectral content of the signal. In this chapter, we will first introduce the reference dataset that will be used to test the framework and then we will describe the features that will be used in the framework. The ND framework will work on the complete collection of features $\mathbf{F} = \{\mathbf{F}_t, \mathbf{F}_f\}$, where \mathbf{F}_t is the collection of time-domain features and \mathbf{F}_f is the collection of frequency-domain features. Some of the features will be extracted for all the signals available, while some others only on a subset of the signals, depending on the settings of the framework, as it will be explained in ??.

1.1 Reference dataset

In the field of ND, a famous bearing vibration dataset has been collected from the Center for Intelligent Maintenance Systems (IMS) of the University of Cincinnati and made available online on the NASA website [1]. Let’s take this as a starting point for our work. The dataset contains the vibration measurements collected at a sampling frequency $f_s = 20\text{kHz}$ of four forced-lubricated bearings. The shaft was kept constant at 2000rpm during the data collection. The test rig is shown in **figure 1.1** and the test parameters are summarized in **table 1.1**, which also shows the type of faults that happened in each repetition of the test.

To visualize what happens to the vibration signal as the bearing degrades over time, let’s consider the “Bearing 3 x” signal from the IMS dataset, shown in **figure 1.2**. The top plot shows the vibration of the new bearing, while the bottom plot shows the vibration of the bearing just before the test was stopped.

It's evident that the degraded signal reaches greater peaks in vibration and has a greater variance. The narrow peaks in the degraded signal are due to the presence of fault frequencies, that are not present in the new bearing signal.

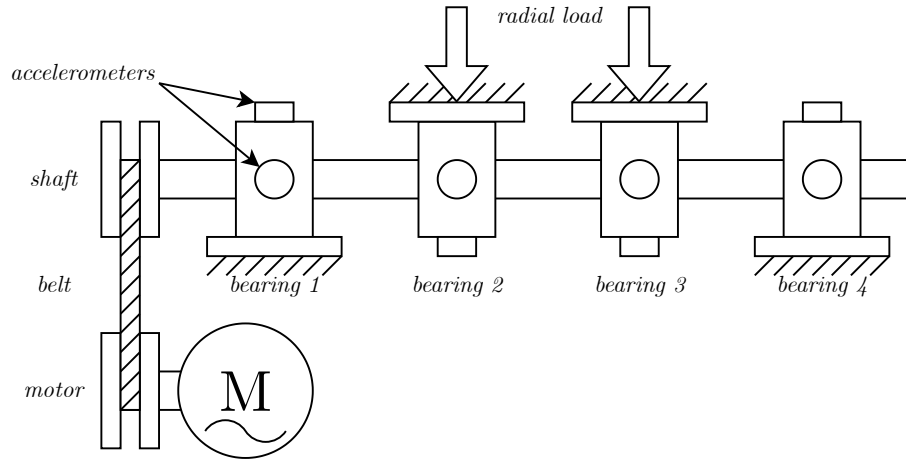


Figure 1.1: The test rig used by [1]

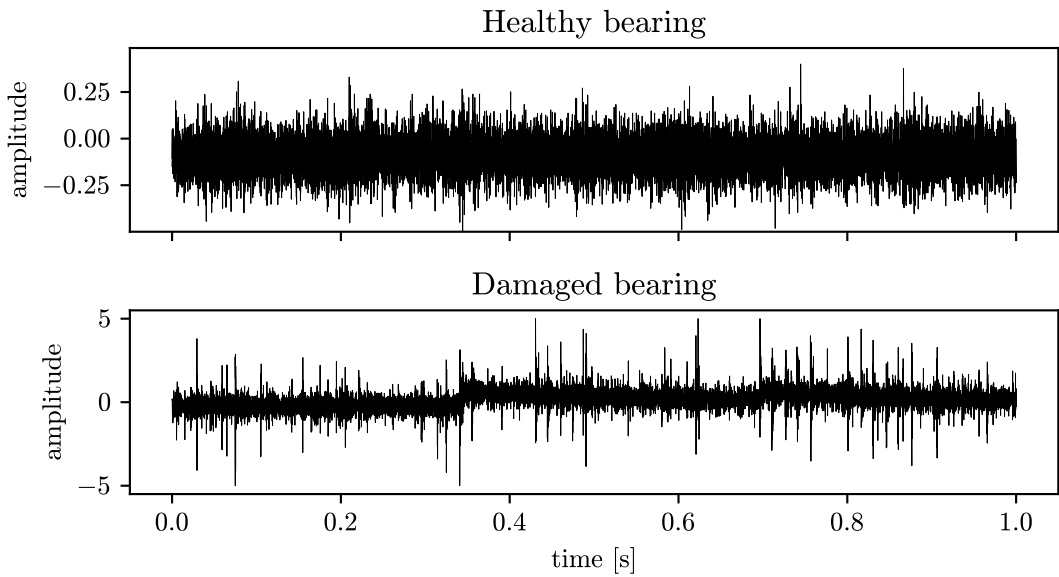


Figure 1.2: "Bearing 3 x" vibration signal from the IMS dataset

Table 1.1: IMS Test setup [1]

	Set No. 1	Set No. 2	Set No. 3
Recording Duration	22/10/2003 - 25/11/2003	12/02/2004 - 19/02/2004	04/03/2004 - 04/04/2004
No. of Files	2156	984	4448
No. of Channels	8	4	4
Channel Arrangement	Bearing 1 ch 1 & 2 Bearing 2 ch 3 & 4 Bearing 3 ch 5 & 6 Bearing 4 ch 7 & 8	Bearing 1 ch 1 Bearing 2 ch 2 Bearing 3 ch 3 Bearing 4 ch 4	Bearing 1 ch 1 Bearing 2 ch 2 Bearing 3 ch 3 Bearing 4 ch 4
File Recording Interval	5 or 10 min	10 min	10 min
Fault type	Bearing 3: inner race defect Bearing 4: roller element defect	Bearing 1: outer race failure	Bearing 3: outer race failure

1.2 Time-domain features

Let's consider a timeserie \mathbf{x} containing n samples x_1, x_2, \dots, x_n . The goal of the feature extraction process is to extract a set of features $\mathbf{F}_t = \{F_1, F_2, \dots, F_m\} \in \mathbb{R}^F$ that can be used to describe the signal. In this section, we will describe the features that will be used in the developed framework.

Mean The first feature to be considered is simply the mean of the signal. It is defined as

$$\mu = \frac{1}{n} \sum_{i=1}^n x_i \quad (1.1)$$

RMS The Root mean square of the signal RMS is related to the power and is defined as

$$\text{RMS} = \sqrt{\frac{1}{n} \sum_{i=1}^n x_i^2} \quad (1.2)$$

Peak-to-peak The peak-to-peak value of the signal is defined as

$$\text{P2P} = \max(\mathbf{x}) - \min(\mathbf{x}) \quad (1.3)$$

Standard deviation The standard deviation is a measure of the dispersion of the signal and is defined w.r.t. a known distribution with knowledge of the true mean μ_{true} as

$$\sigma = \sqrt{\frac{1}{n} \sum_{i=1}^n (x_i - \mu_{true})^2} \quad (1.4)$$

but since in our case we don't know the true mean, we will use the sampled standard deviation, which is the best estimate, defined as

$$\hat{\sigma} = \sqrt{\frac{1}{n-1} \sum_{i=1}^n (x_i - \mu)^2} \quad (1.5)$$

Skewness The skewness is a measure of the asymmetry of the signal and is defined as

$$\gamma = \mathbb{E} \left[\left(\frac{x - \mu}{\sigma} \right)^3 \right] \quad (1.6)$$

and can be estimated on sampled data as

$$\hat{\gamma} = \frac{\sqrt{n(n-1)}}{n-2} \frac{\frac{1}{n} \sum_{i=1}^n (x_i - \bar{x})^3}{\left[\frac{1}{n} \sum_{i=1}^n (x_i - \bar{x})^2 \right]^{3/2}} \quad (1.7)$$

Kurtosis The kurtosis is a measure of the “peakedness” of the signal and is defined as

$$\kappa = \frac{1}{n} \sum_{i=1}^n \left(\frac{x_i - \mu_{true}}{\sigma} \right)^4 \quad (1.8)$$

It can be estimated on sampled data as

$$\hat{\kappa} = \frac{(n+1)n}{(n-1)(n-2)(n-3)} \frac{\sum_{i=1}^n (x_i - \mu)^4}{k_2^2} - 3 \frac{(n-1)^2}{(n-2)(n-3)} \quad (1.9)$$

To visualize the evolution of the features over time, consider all the snapshots of the “Bearing 3 x” signal from the IMS dataset and plot all the time-domain features described above. The result is shown in **figure 1.3**. Having seen also **figure 1.2**, it's not surprising that the P2P and the kurtosis are the time domain features that capture the degradation of the bearing the earliest.

1.3 Frequency-domain features

To capture also the frequency behaviour of the signal, other tools are needed. In this section, we will describe the frequency-domain features $\mathbf{F}_f = \{F_{m+1}, F_{m+2}, \dots, F_l\}$ that will be used in the developed framework.

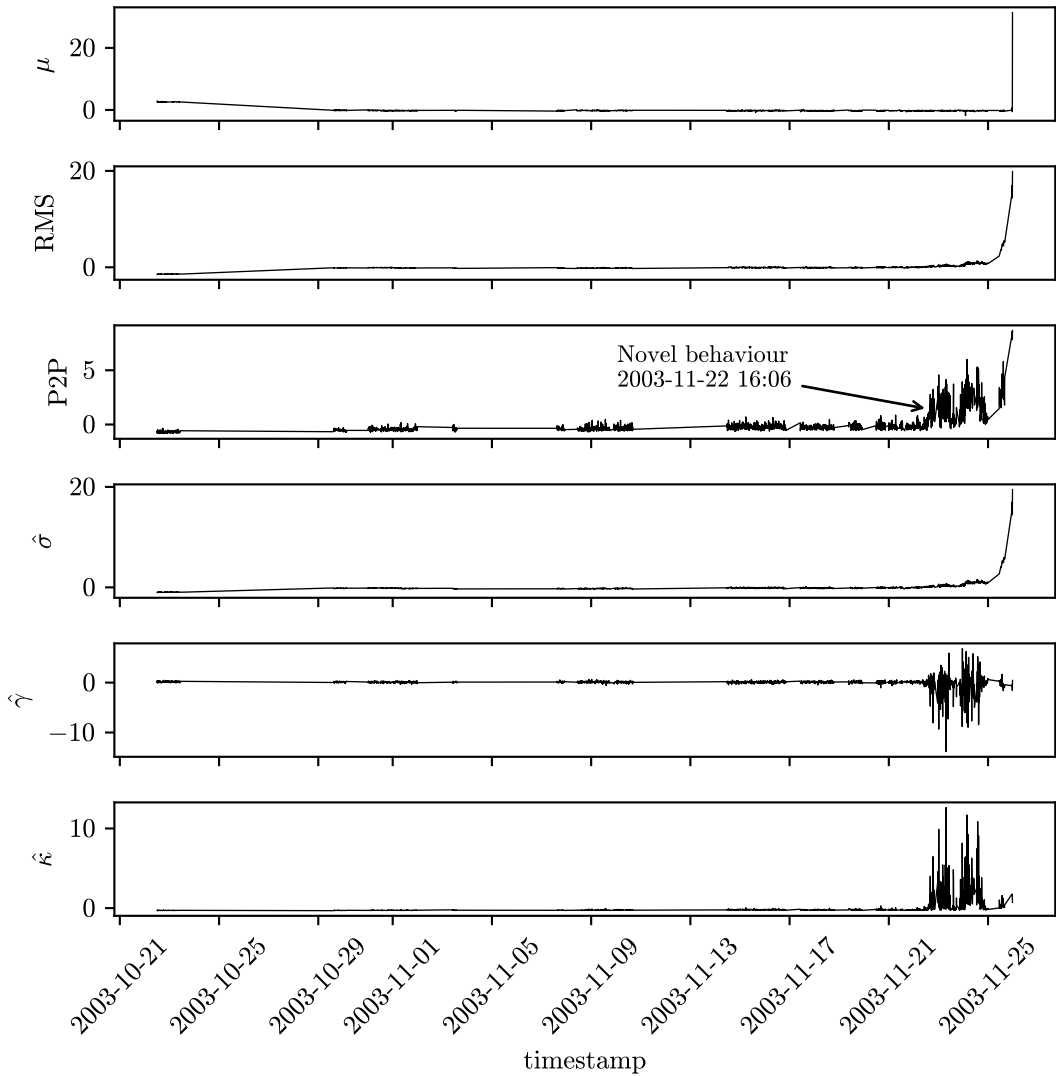


Figure 1.3: All time-domain features for the “Bearing 3 x” vibration signal from the IMS dataset

1.3.1 Fourier Transform

One powerful tool to analyze the frequency content of a signal is the Fourier transform or, in the case of a discrete signal, the Discrete Fourier Transform(DFT), which has a very efficient implementation in the Fast Fourier Transform (FFT) algorithm [2]. This algorithm is implemented in many programming languages and libraries, including python and C. The theory behind this topic is briefly described

in ??.

To have a better understanding of the capability of the FFT to capture the frequency content of a signal (and the presence of a disturbance in a portion of the signal), consider the following signal, composed by the sum of four sinusoids with different frequencies that are plotted with its DFT in **figure 1.4**:

$$x(t) = \sin(2\pi f_1 t) + \sin(2\pi f_2 t) + \sin(2\pi f_3 t) + \sin(2\pi f_4 t), \\ t \in [0, 1], \quad \{f_1, f_2, f_3, f_4\} = \{2, 5, 7, 15\} \text{Hz} \quad (1.10)$$

In the **figure 1.4** it is possible to see the four peaks in the frequency domain, corresponding to the four frequencies of the sinusoids. Now, consider the same signal, but with an additive disturbance in a small portion of the signal, as shown in **figure 1.5**. The disturbance is a period of the signal $x(t) = \sin(2\pi f_5 t)$, with $f_5 = 50 \text{Hz}$, that is added to the signal in the interval $t \in [0.4, 0.6]$. The DFT of this signal is shown in **figure 1.5**. It is possible to see that the disturbance is captured by the spectrum as a broad frequency additional components, instead of a peak at $f_5 = 50 \text{Hz}$. This is because the disturbance is not acting on the whole signal. For our purpose, this is still good because we can detect the variation of all the frequencies involved.

Consider the period of the undisturbed signal, that is the LCM of the periods of the four sinusoids composing the signal.

$$T = \text{LCM}\left(\frac{1}{2}\text{s}, \frac{1}{5}\text{s}, \frac{1}{7}\text{s}, \frac{1}{15}\text{s}\right) = 1\text{s}$$

So, we were processing a signal that has a period of one second, sampled for exactly one second. Let's see what happens if we sample the same signal for a time that is not an integer multiple of the period. In **figure 1.6** it is shown the DFT of the same signal as before, but sampled for $t \in [0, 0.9]$. It is possible to see that the peaks are still at the frequencies of the sinusoids composing the signal, but they are not single points as it appears that also frequencies near the true frequencies are present. This phenomenon is called *spectral leakage* and happens because the signal is not sampled for an integer number of periods [3].

Preprocessing

Up to now, it has been shown that the DFT will translate the presence of a disturbance in the time domain into several periodic components in the frequency domain. However, it has the spectral leakage weakness if the sampling interval is not an integer multiple of the period of the signal which is the most likely scenario in a real application. To compensate for this phenomenon, it is better to use a transformation to the signal that makes it artificially start and end with the same

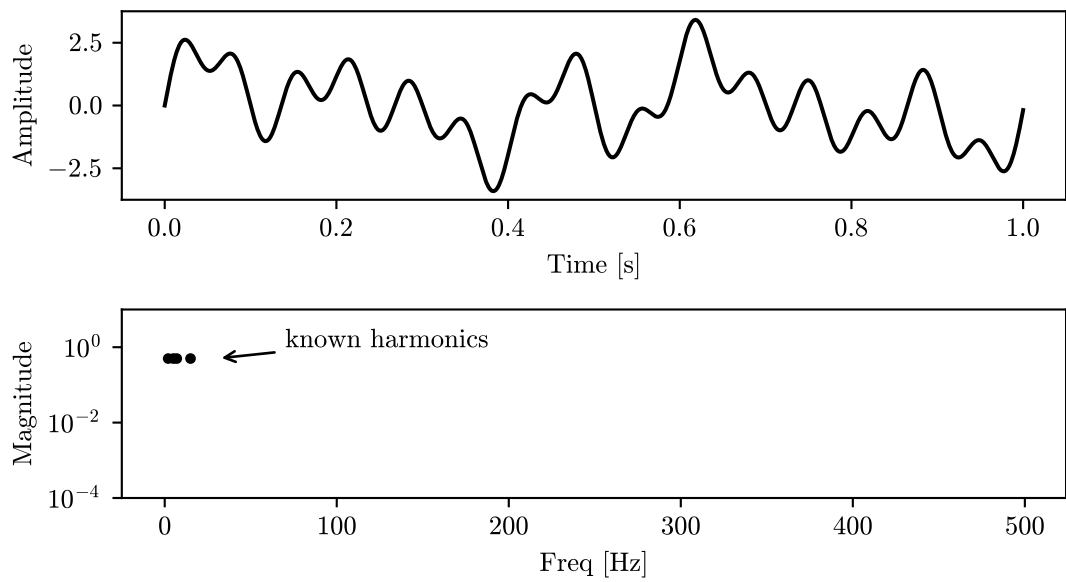


Figure 1.4: FFT of the signal with known frequency components

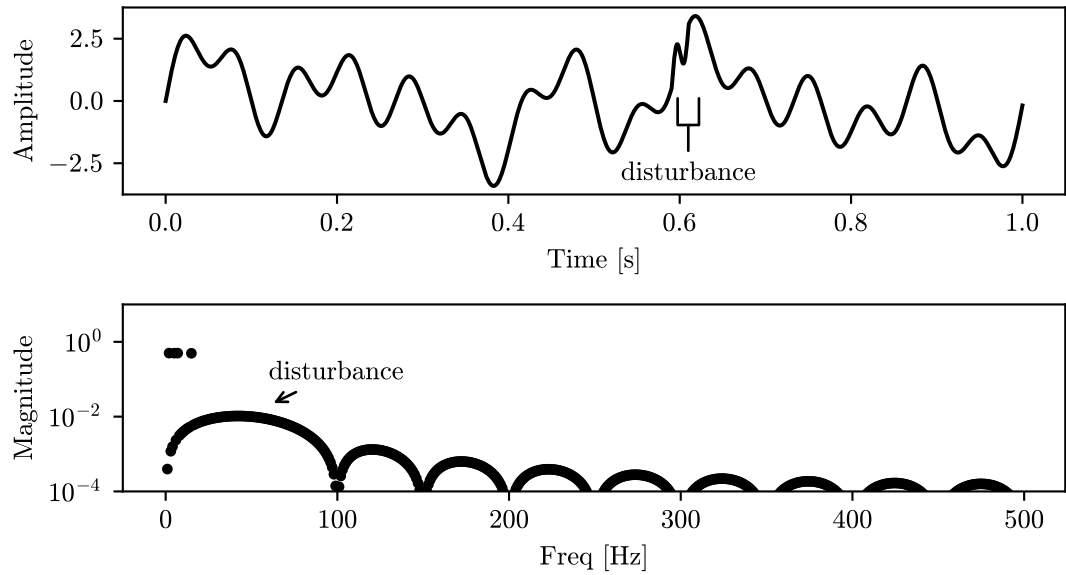


Figure 1.5: FFT of the signal with known frequency components, and an additive disturbance

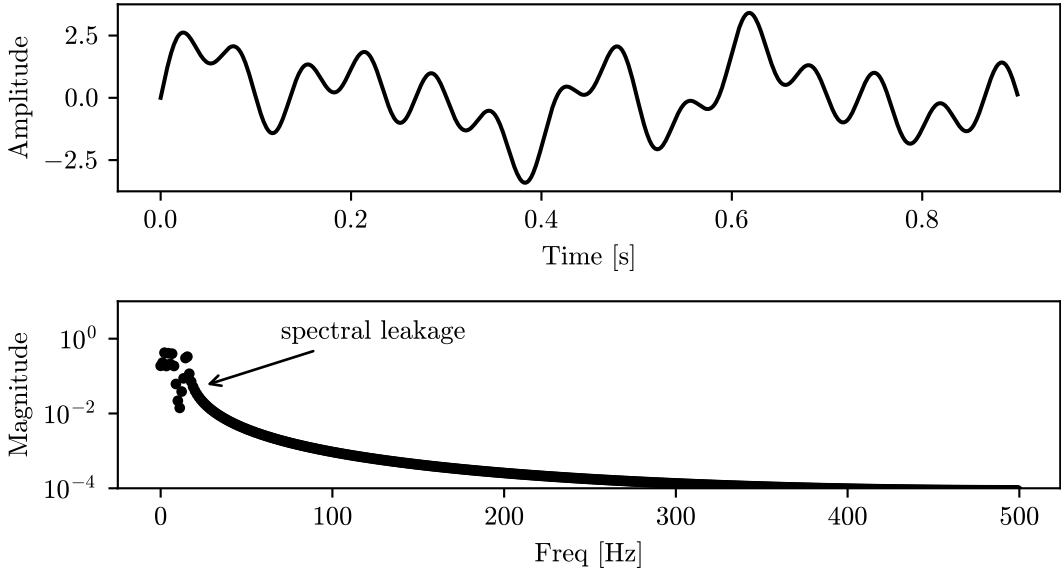


Figure 1.6: FFT of the signal with known frequency components, with a domain that is not an integer multiple of the period

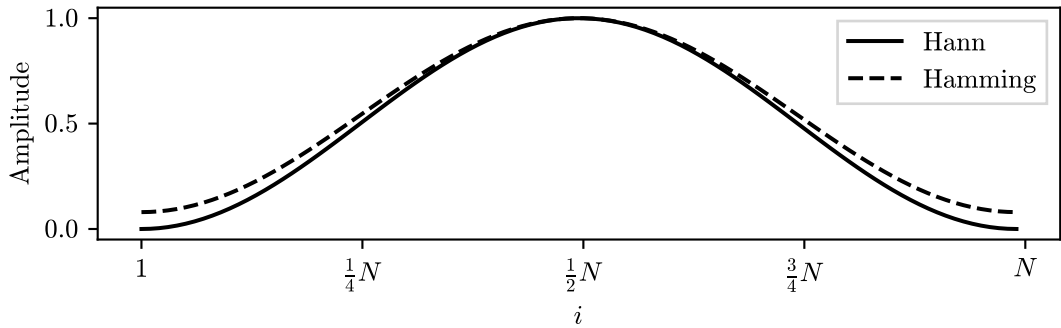


Figure 1.7: Hann and Hamming windows

value. This can be done with a *windowing* function, or with the *flip and reverse* method [4].

The most common windowing functions are the *Hann* and the *Hamming* windows, defined as:

$$w_{\text{hann}}(i) = 0.5 \left[1 - \cos \left(\frac{2\pi i}{n} \right) \right] \quad (1.11)$$

$$w_{\text{hamming}}(i) = \frac{25}{46} \left[1 - \cos \left(\frac{2\pi i}{n} \right) \right] \quad (1.12)$$

where i is the considered sample as the independent variable and n is the total number of samples. Those functions are plotted in **figure 1.7**. The preprocessing operation is simply to multiply the signal by the windowing function. this will make the first and last point of the signal exactly zero in the case of the Hann window, and very close to zero in the case of the Hamming window but with the advantage of having a narrower peak in the spectrum.

The “flip and reverse” method is simply to concatenate a flipped copy of the signal to itself and downsampling it to preserve the original length of the array, as follows [4]:

$$x_{new}(i) = \begin{cases} x(2i) & \text{if } i \leq \frac{n}{2} \\ x(2(n-i)) & \text{if } i > \frac{n}{2} \end{cases} \quad \forall i \in [1, n] \quad (1.13)$$

A comparison of those preprocessing techniques is shown in **figure 1.8** and **figure 1.9**. In both figures, it is evident that the “flip and reverse” method generates a fake peak at half the sampling frequency, while the windowing function doesn't. Moreover, looking at **figure 1.9**, it is possible to see that the Hann window better suppresses the spectral leakage. In figure **figure 1.10** it is shown the effect of different preprocessing techniques on a real-world signal from the IMS dataset. The Hann window will be implicitly used in the rest of this section.

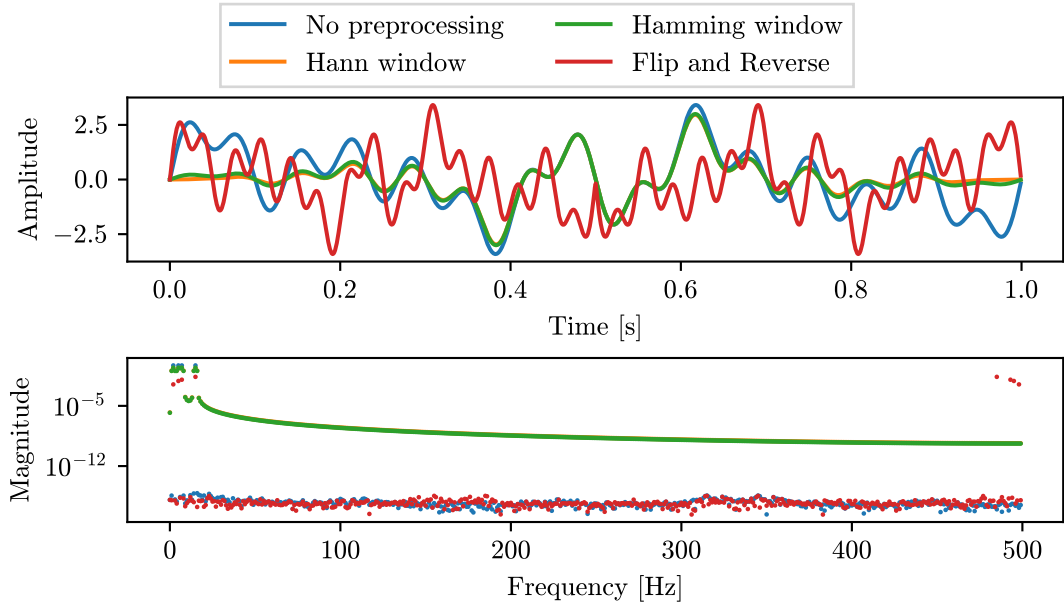


Figure 1.8: FFT of the signal with a domain that is an integer multiple of the period, and preprocessing techniques applied

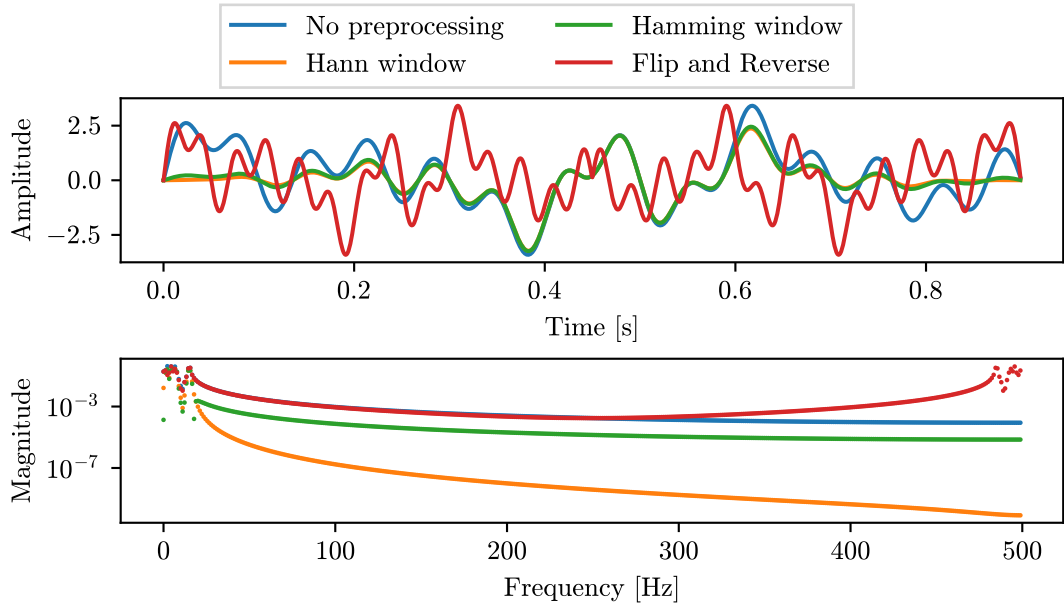


Figure 1.9: FFT of the signal with a domain that is not an integer multiple of the period, and preprocessing techniques applied

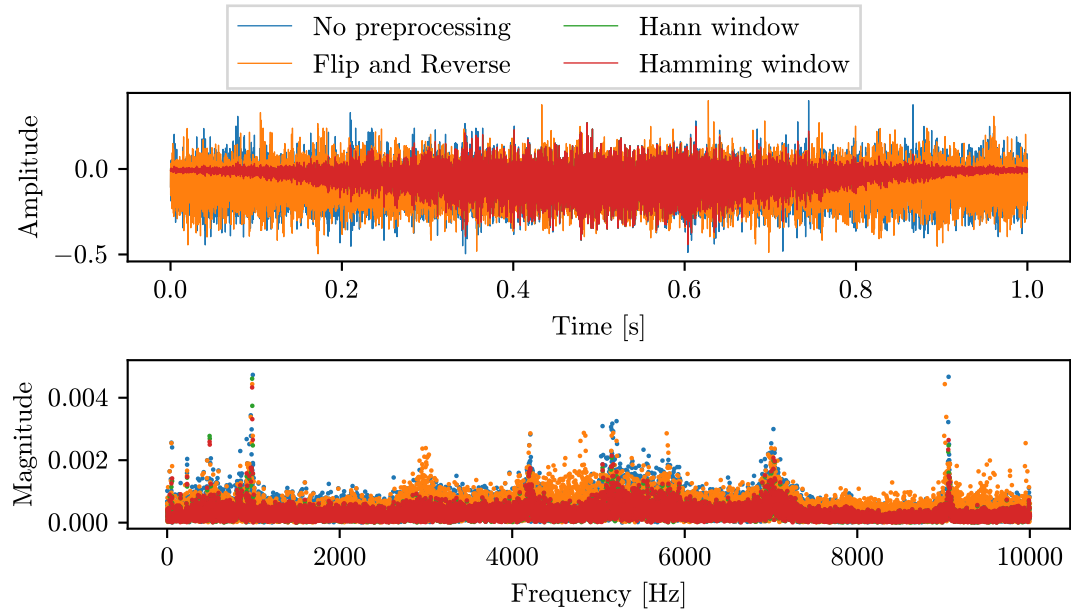


Figure 1.10: FFT of the “Bearing 3 x” vibration signal from the IMS dataset, in normal conditions, with preprocessing techniques applied

Application to the reference dataset

At this point, to see if the spectrum is representative of a fault, as it has been done for the time-domain features, we can plot all the spectrum for all the snapshots of the “Bearing 3 x” signal from the IMS dataset, as shown in **figure 1.11**. Looking at the picture, we can see that the signature frequencies of faults are present in the spectrum, and they become more and more prominent as the bearing degrades. This is a good sign justifying to use of the spectrum to detect the novel behaviour.

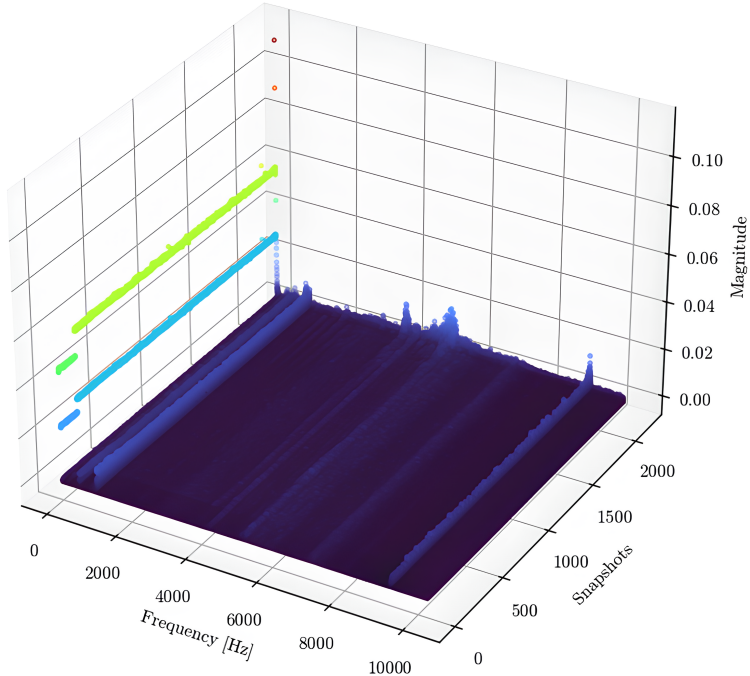


Figure 1.11: FFT of the “Bearing 3 x” vibration signal from the IMS dataset, in normal conditions with Hann window preprocessing applied

1.3.2 Wavelet Packet Decomposition

Motivation

In the previous **subsection 1.3.1**, it has been shown that the spectrum of the signal contains useful information for performing ND. Remembering that the ultimate scope of this work is to develop a framework that runs in edge computing, it is important to consider the computational cost of the features extraction, and the memory usage. Considering only the FFT of all signals of the dataset shown in **figure 1.11** and the fact that a floating point value uses 64 bit, the memory

usage is $64\text{bit} \times 10\text{kFeatures} \times 2156\text{Snapshots} \div 8\text{bit}/\text{byte} \approx 172.5\text{Mb}$. This is not a big problem for a desktop computer, but it may be a problem for an IOT device. Moreover, the FFT is a very computationally expensive operation, with a complexity of $\mathcal{O}(n \log n)$, where n is the number of samples.

To overcome this problem it is necessary to find a method that exploits the same information in the frequency domain, but using much less computational power and memory. Other tools for the frequency analysis are the Wavelet Transform and, in particular, the Wavelet Packet Decomposition (WPD) has been used in the developed framework. The theory behind this topic is briefly described in ??.

Furthermore, most ML algorithms perform better with a lower number of features, and the WPD is able to extract a lower number of features. For example, for a signal like the ones in the IMS dataset $\boldsymbol{x} \in \mathbb{R}^{2000}$, the WPD with a depth of 6 will output $2^6 = 64$ coefficients, which are transformed into features. On the other hand, the FFT will output 2000 coefficients, which can already be considered a high dimensionality space.

Application to the reference dataset

At this point, let's consider a WPD with a depth of 6, that outputs $2^6 = 64$ coefficients. We are going to take the norm of each coefficient as a feature so, in the end, we will have 64 features (from “aaaaaa” that leads from all the approximation coefficients to “dddddd” that leads from all the detail coefficients instead, passing for all the combinations in between). The WPD of the “Bearing 3 x” signal from the IMS dataset is shown in **figure 1.12** as the bearing is new, and in **figure 1.13** as the bearing is degraded. It is possible to see that the WPD is able to capture the presence of the fault frequencies.

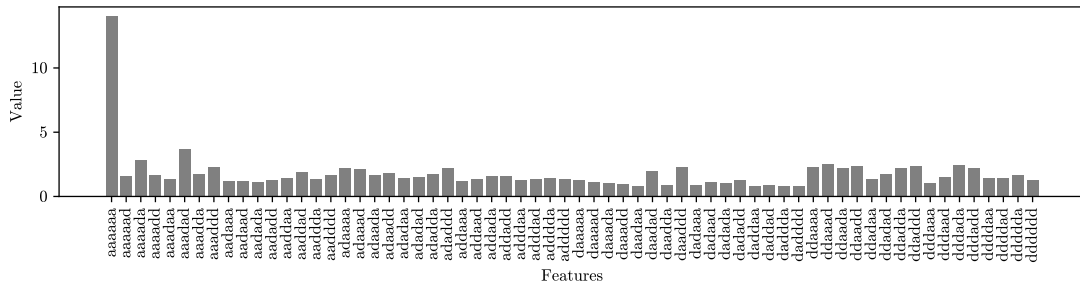


Figure 1.12: Wavelet Packet Decomposition of the “Bearing 3 x” vibration signal from the IMS dataset, in normal conditions

At this point, it is possible to extract the features with the WPD and plot them over time, for the whole dataset, as it has been done for the FFT in **figure 1.11**. The result is shown in **figure 1.14**. The memory consumption of the data in the

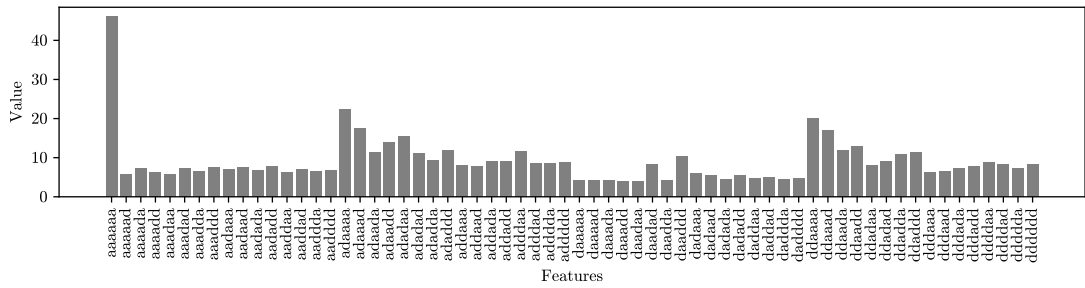


Figure 1.13: Wavelet Packet Decomposition of the “Bearing 3 x” vibration signal from the IMS dataset, in abnormal conditions

second figure is $64\text{bit} \times 64\text{Features} \times 2156\text{Snapshots} \div 8\text{bit}/\text{byte} \approx 1.1\text{Mb}$, that means that the memory saving obtained using WPD instead of FFT exceeds 99%. Despite this huge memory saving, it is possible to see that the WPD is able to retain the information about the fault frequencies, and it is possible to see that the fault frequencies become more and more prominent as the bearing degrades over time. For this reason, the WPD will be used in the developed framework, along with the time-domain features.

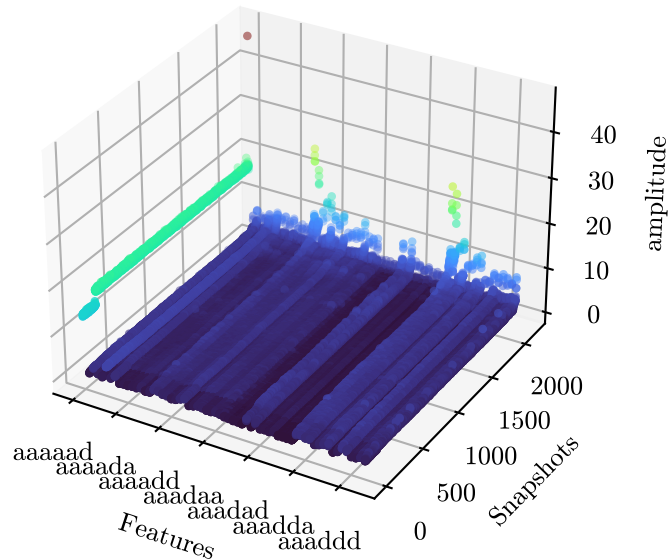


Figure 1.14: Wavelet Packet Decomposition of the “Bearing 3 x” vibration signal from the IMS dataset, in normal conditions

1.4 Conclusions

Even just considering very simple time-domain features, we can already detect the degradation of the bearing by comparing these feature values to a threshold. On the other hand, also the frequency-domain features could be just compared with a threshold to detect novel behaviours. But, as we will see in ??, a general purpose framework based upon a more sophisticated approach based on the clustering of the data, it will be possible to condense all the features from all the signals into a single metric that will be used to detect the novel behaviour. This will have several advantages. Some of them are being able to detect a novel behaviour even if it is not possible to define a threshold for each feature, and the single threshold to be defined on the metric will be easier to interpret and tune. Moreover, the framework will be able to detect the novelty even earlier and even if the degradation of the bearing is not captured by the time-domain features, but only by the frequency-domain features.

Bibliography

- [1] J. Lee, H. Qiu, G. Yu, J. Lin, and Rexnord Technical Services. «Bearing Data Set». In: *IMS, University of Cincinnati* (2007). Available at: <https://www.nasa.gov/intelligent-systems-division/discovery-and-systems-health/pcoe/pcoe-data-set-repository/> (cit. on pp. 1–3).
- [2] James W Cooley and John W Tukey. «An algorithm for the machine calculation of complex Fourier series». In: *Mathematics of computation* 19.90 (1965), pp. 297–301 (cit. on p. 5).
- [3] Arvid Breitenbach. «Against spectral leakage». In: *Measurement* 25.2 (1999), pp. 135–142. ISSN: 0263-2241. DOI: [https://doi.org/10.1016/S0263-2241\(98\)00074-8](https://doi.org/10.1016/S0263-2241(98)00074-8). URL: <https://www.sciencedirect.com/science/article/pii/S0263224198000748> (cit. on p. 6).
- [4] Chao-Yen Wu and A.Terry Bahill. «Preprocessing methods in the computation of the fast fourier transform». In: *Computers & Industrial Engineering* 21.1 (1991), pp. 653–657. ISSN: 0360-8352. DOI: [https://doi.org/10.1016/0360-8352\(91\)90168-6](https://doi.org/10.1016/0360-8352(91)90168-6). URL: <https://www.sciencedirect.com/science/article/pii/0360835291901686> (cit. on pp. 8, 9).